Macromolecules

Article

pubs.acs.org/Macromolecules

Viscoelasticity of Poly(ethylene glycol) Solutions on Supported Lipid Bilayers via Quartz Crystal Microbalance with Dissipation

Ziliang Zhao,[†,§] Xiangling Ji,[*,†] Rumiana Dimova,[‡] Reinhard Lipowsky,[‡] and Yonggang Liu[*,†,‡]

[†]State Key Laboratory of Polymer Physics and Chemistry, Changchun Institute of Applied Chemistry, Chinese Academy of Sciences, 130022 Changchun, China

[‡]Department of Theory and Bio-Systems, Max Planck Institute of Colloids and Interfaces, Science Park Golm, 14424 Potsdam, Germany

[§]University of Chinese Academy of Sciences, 100049 Beijing, China

Supporting Information

ABSTRACT: Supported lipid bilayers of 1,2-dioleoyl-*sn*-glycero-3-phosphocholine were formed on a silicon oxide substrate, and the viscoelasticity of poly(ethylene glycol) (PEG) solutions above the bilayer was subsequently studied by quartz crystal microbalance with dissipation monitoring. No detectable adsorption of PEG molecules to the bilayer was found over a broad range of PEG molecular weight at various concentrations. The viscoelastic properties of the PEG solutions were obtained from the shifts in the resonance frequency and the energy dissipation factor of the polymer solution in contact with the resonator-supported lipid bilayer. The resulting viscoelastic properties of PEG solutions were found to be in excellent agreement with the Zimm model for linear polymer chains in a good solvent. The excluded volume scaling exponent ν for PEG in water shows an ideal-to-real crossover with increasing molecular weight. The exponent adopts a value of 0.50 for short chains and gradually increases to 0.565 for long chains. The onset of the excluded volume effect of PEG in water, a good solvent, lies in the molecular weight range between 4000 and 8000.

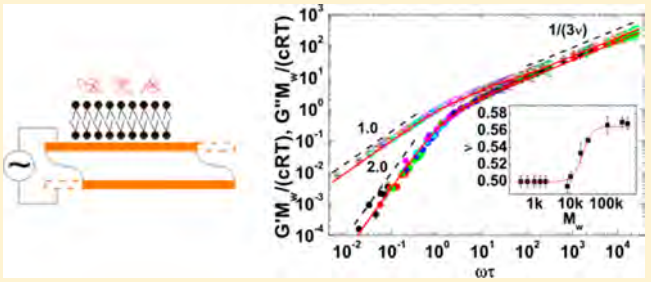

INTRODUCTION

Viscoelasticity of polymer solutions has been the subject of intensive research for several decades, which provides considerable insights into the dynamics of polymer chains in both dilute and concentrated regimes.[1,2] Polymer solutions usually have a wide spectrum of relaxation times which is not easy to probe experimentally. Thus, it is necessary to employ instrumentation operating at frequencies capable of probing the whole relaxation time spectrum. However, commercial rheometers employing oscillatory shear flows generated by cone-and-plate, parallel-plate, or tube geometries have a typical upper frequency limit of about 100 Hz, which is not high enough unless for high molecular weight polymers in a very viscous solvent. Such a frequency limitation can often be circumvented by employing time−temperature superposition (TTS) for polymer solutions with good solvent conditions for which the viscosity exhibits a strong dependence on temperature.[1] However, TTS is not so effective for aqueous polymer solutions because the viscosity of water weakly depends on temperature and water represents a good solvent only over a limited temperature range depending on the polymer species. Additionally, theories of polymer dynamics in solutions and melts predict explicit scaling behaviors at high frequencies,[3−6] which depend on the chain architectures, the flexibility of the chains, and the solvent−polymer interactions. Therefore, it is highly desirable to use experimental methods that can probe the polymer dynamics in the high-frequency regime.

Diffusing wave spectroscopy can measure the viscoelasticity of polymer solutions up to frequencies of about 100 kHz[7] but is not applicable, in general, to dilute polymer solutions. Instruments based on the torsional resonator, which was pioneered by Mason,[8] have been used to study the viscoelasticity of polymer solutions up to hundreds of kilohertz.[9−11] Another potential technique to probe the viscoelasticity of polymer solution at high frequency is the quartz crystal microbalance with dissipation (QCM-D). QCM was initially employed in air to measure the mass deposited on a piezoelectric resonator according to the decrease of the oscillation frequency[12] and was later applied in liquid environments.[13−15] Similar to torsional resonators which are working in the kilohertz range, QCM-D measures both resonance frequency and bandwidth (or energy dissipation factor) of the resonator in contact with the fluids, from which one can deduce the viscosity of Newtonian fluids in the megahertz frequency range.[16] It is expected that QCM-D can also measure the viscoelasticity of polymer solutions as

Received: January 16, 2015
Revised: February 23, 2015

DOI: 10.1021/acs.macromol.5b00095
Macromolecules XXXX, XXX, XXX−XXX

torsional resonator did but at higher frequencies.[16−19] However, it should be noted that the mass sensitivity constant of the adsorption on the resonator is inversely proportional to the square of the fundamental resonance frequency. Therefore, the perturbations arising from polymer adsorption on the resonator should be minimized in order to probe the viscoelasticity of polymer solutions by QCM-D. This can be achieved by coating the resonator surface with an inert layer,[20−22] such as a gold film, a polymer layer, or a self-assembled monolayer or bilayer, which should be rigid and does not cause adsorption of the studied polymer molecules. Recent studies by Zhu et al. discussed the viscosity and shear modulus of poly(ethylene glycol) (PEG) solutions near a gold-coated 5 MHz resonator, but unfortunately the high-frequency character of the QCM-D results was not considered.[20] Coating the quartz crystal resonator with a supported lipid bilayer[22] (SLB) is a convenient and promising way to provide a nonadsorbing interface for water-soluble polymers such as PEG and dextran. PEG had been used for aggregating or fusing vesicles and cells, which is believed to be governed by attraction induced by polymer depletion from the vesicle membranes.[23,24] The static and hydrodynamic forces between two substrate-supported lipid bilayers in PEG solution have been studied by surface force apparatus, and a crossover from depletion attraction to adsorption with increasing molecular weight of PEG was observed.[25] Recent studies on giant unilamellar vesicles enclosing an aqueous solution of PEG and dextran revealed the formation of nanotubes[26] and budding transformations,[27] two processes that depend on the membranes' spontaneous curvature that can be generated by depletion layers of the dissolved polymers, as first predicted in ref 28. Therefore, for PEG solutions in contact with the SLB-coated quartz crystal resonator, it is expected that PEG is depleted from the surface and that the resonator primarily probes the viscoelasticity of the solution because the thickness of the depletion layer is much smaller than the viscous penetration depth of the resonator.

In the present paper, we study the formation of the SLB on silicon oxide substrates followed by an investigation of the viscoelastic properties of aqueous PEG solution in contact with the SLB using QCM-D in the high-frequency regime of 5−65 MHz. The results are compared with the frame of the Zimm model for linear polymer chains in a good solvent.

MATERIALS AND METHODS

Materials. 1,2-Dioleoyl-*sn*-glycero-3-phosphocholine (DOPC) was purchased from Avanti Polar Lipids Inc. and used without further purification; the lipids were stored at −20 °C upon arrival. PEGs of different molecular weights (M_w = 200, 400, 600, 1000, 1400, 2000, 4000, 6000, 8000, 10 000, 20 000, and 35 000) were obtained from Sigma-Aldrich; they were desiccated in vacuum until no further reduction in mass was observed before use. The polydispersities M_w/M_n of these PEG samples are less than 1.1, according to gel permeation chromatography measurement (Supporting Information Table S1). Poly(ethylene oxide)s (PEOs), synonymous to PEG, with higher molecular weight of 116 000, 278 000, and 443 000 were obtained from Polymer Laboratories Ltd. All other reagents were of analytical grade. All solutions were prepared using ultrapure water from Sartorius water purification system with a resistivity of 18.2 MΩ·cm.

Preparation and Characterization of Liposomes. The liposomes were prepared by the extrusion method.[29] About 400 μL DOPC chloroform solution (concentration 10 mg/mL) was dried under a gentle stream of nitrogen gas onto the walls of a continuously rolled vial followed by desiccating in vacuum for 3 h to completely remove the solvent. The dried lipid film was then hydrated by adding 2 mL aqueous solution containing 150 mM NaCl under gentle vortexing. Large unilamellar vesicles (LUVs) were obtained by extruding the solution 31 times through a polycarbonate membrane with a pore size of 100 nm via a mini-extruder (Avanti Polar Lipids Inc.). The obtained liposomes have a narrow size distribution with averaged diameter of 122 ± 2 nm, as determined by a Malvern Zetasizer Nano ZS90 dynamic light scattering instrument. Vesicle suspensions were stored at 4 °C and diluted to a lipid concentration of 0.1 mg/mL prior to use.

QCM-D. The adsorption kinetics and the properties of the adsorbed layer were monitored on a Q-Sense E4 system (Biolin Scientific, Sweden).[30] The AT-cut quartz crystal sensors with a fundamental resonance frequency of 4.95 MHz were cleaned with two cycles of the following procedure before each usage: soaked in 2% SDS solution for 30 min, rinsed with ultrapure water, blow-dried with nitrogen gas, and exposed to an ultraviolet (UV)/ozone cleaner for 15 min.[22] QCM-D experiments were carried out at 24 ± 0.02 °C in an exchange mode at a flow rate of 100 μL/min. At least 1.0 mL of degassed sample solution was delivered into the chamber containing the sensor crystal (internal volume 40 μL) to ensure a complete exchange of the liquid. The shifts in the resonant frequency (Δf_n) and the energy dissipation factor (ΔD_n) of the sensors were acquired simultaneously at multiple harmonics (overtone number n = 1, 3, 5, 7, 9, 11, and 13).

The measurements were performed after mounting the crystals in the flow module and establishing a baseline with a buffer containing 150 mM NaCl solution. DOPC vesicle solution was pumped into the chamber to form the supported lipid bilayers on the crystal surface, followed by rinsing with the above buffer again. The buffer was exchanged to water, before aqueous solution of PEG was pumped into the chamber. The adsorption behavior of PEG solution of different molecular weights at various concentrations on the SLB was checked one after another, and a sufficient amount of water was used to rinse the SLB surface between each step. For comparison, the adsorption behavior of sucrose solution of different concentrations on the SLB was also studied in the same way.

For a thin and rigid film attached to the substrate, the Sauerbrey equation describes the relationship between the frequency shift Δf_n and the adsorbed mass Δm.[12] This equation has the form

$$\Delta m = -\frac{(\rho_q \mu_q)^{1/2}}{2f_0^{\,2}}\frac{\Delta f_n}{n} = -C\frac{\Delta f_n}{n} \tag{1}$$

where f_0 is the fundamental resonance frequency of the sensor (4.95 MHz), ρ_q is the density of quartz (2.648 g/cm^3), μ_q is the shear modulus of the crystal (2.947×10^{11} g cm^{-1} s^{-2}), and C is the mass sensitivity constant (18.0 ng cm^{-2} Hz^{-1} at f_0 = 4.95 MHz). For Sauerbrey films, the frequency shift Δf_n is proportional to the overtone number n and the dissipation shift $\Delta D_n \sim 0$. However, a soft and viscous adlayer will dissipate energy and damp the sensor oscillation. In this case, one can get information about the stiffness of the adlayer from the shift in the energy dissipation factor, which is defined as the energy dissipated per oscillation divided by the total energy stored in the oscillator.

Density and Viscosity Measurements. The density of each solution was measured at 24 ± 0.01 °C by a DMA 4500M density meter (Anton Paar) with a resolution of 5×10^{-5} g/mL. The viscosities of the solutions were determined by a stress-controlled rheometer ARES-G2 (TA Instruments) with a cone-and-plate geometry (with a cone diameter of 5 cm and a cone angle of 2.2°). The measurements were performed in steady flow mode with a shear rate between 1 and 100 s^{-1} at 24 ± 0.1 °C by circulating water under the lower steel plate.

RESULTS AND DISCUSSION

Formation of the DOPC SLB. Figure 1 shows the formation of a supported lipid bilayer from DOPC LUVs with an average size of 122 ± 2 nm on a silicon oxide substrate as monitored by QCM-D. After establishing the baseline with buffer for about 5 min, DOPC liposome solution was pumped

DOI: 10.1021/acs.macromol.5b00095
Macromolecules XXXX, XXX, XXX−XXX

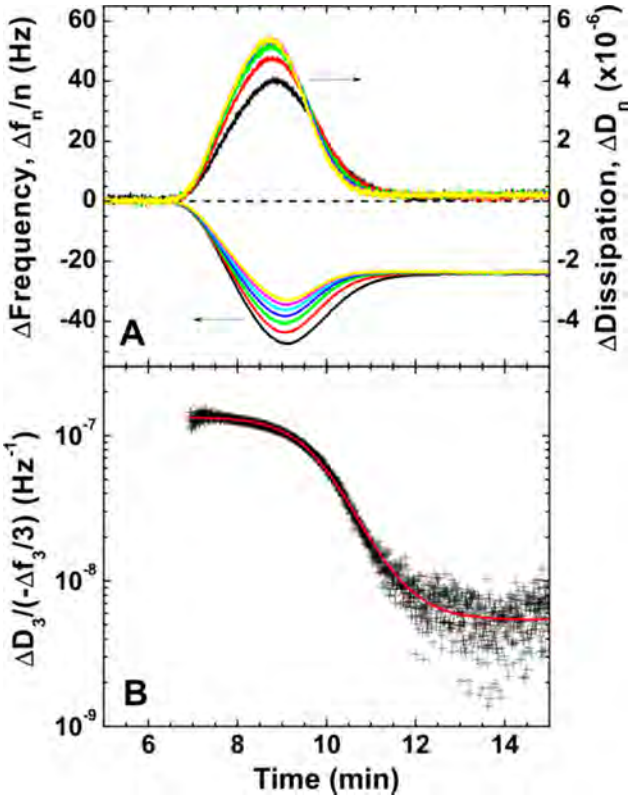

Figure 1. Formation of the DOPC SLB on a silicon oxide substrate monitored by QCM-D. (A) Resonance frequency shifts $\Delta f_n/n$ and energy dissipation shifts ΔD_n for all seven harmonics as a function of time. The frequency signals from bottom to top are for overtone number n = 1, 3, 5, 7, 9, 11, and 13, respectively. The corresponding dissipation signals at each overtone are shown with the same color as frequency. The black dashed line is a guide to the eyes with a value of 0 for the baseline. (B) Ratio of the dissipation shift to the frequency shift for the third overtone, $\Delta D_3/(-\Delta f_3/3)$, as a function of time.

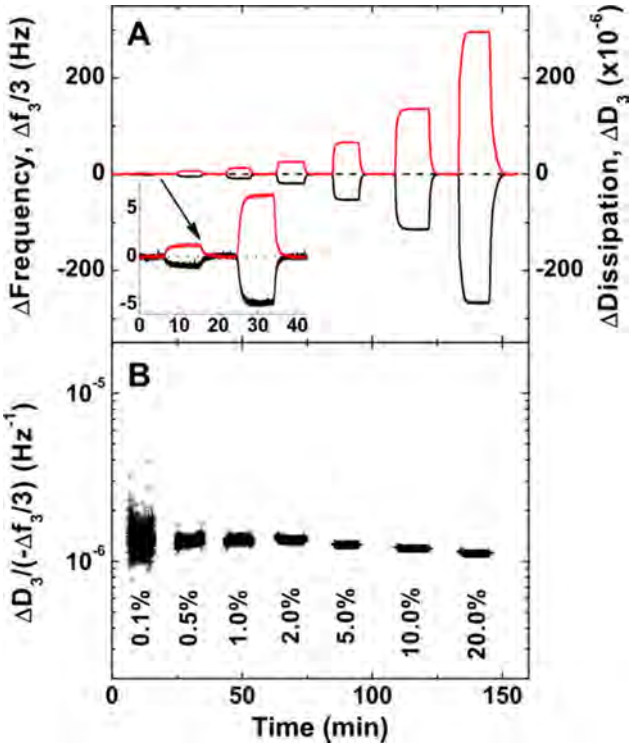

Figure 2. QCM-D signals for a series of subsequent experiments, in which the SLB was exposed to aqueous solutions with different concentration of PEG-8000, interrupted by rinsing the SLB with water. The signals from left to right are for 0.1, 0.5, 1.0, 2.0, 5.0, 10.0, and 20.0% PEG solutions, respectively. The time evolutions of the frequency shift $\Delta f_3/3$ (black curve) and the dissipation shift ΔD_3 (red curve) and their ratio $\Delta D_3/(-\Delta f_3/3)$ are shown in (A) and (B), respectively. The signals for 0.1 and 0.5% PEG in (A) are enlarged and shown as an inset. The black dashed line is a guide to the eyes with a value of 0 for the baseline.

into the chamber at 6.7 min; a decrease of the resonance frequency and an increase of the energy dissipation factor were observed, caused by the deposition of liposomes on the hydrophilic substrate. The frequency shifts, $\Delta f_n/n$, decreased to values between −47 and −33 Hz (the value is different for each overtone) at 9.1 min, before the signals reached a plateau value of −24 Hz (the value is the same for all harmonics) after 13.0 min. This is due to the rupture of adsorbed liposomes to form supported lipid bilayers and the release of trapped water. The corresponding dissipation shifts, ΔD_n, reached n-dependent maxima of about 5.0×10^{-6} for the adsorbed liposomes before stabilizing at n-independent values of $(0.1–0.2) \times 10^{-6}$ for the rigid bilayers. The ratio between the dissipation shift and the frequency shift $\Delta D_n/(-\Delta f_n/n)$ showed a transition from a value more than 10^{-7} Hz^{-1} for the "soft" liposomes to a value less than 10^{-8} Hz^{-1} for the "rigid" bilayers. The scenario of vesicle adsorption followed by rupture observed by QCM-D is in good agreement with previous observations in different experiments and is supported by the theory.[22,30−37]

PEG Solutions in Contact with the SLB-Coated Resonator. After the DOPC bilayer had been formed on the resonator substrate, aqueous PEG solution was subsequently brought into contact with the DOPC SLB. Figure 2 shows the time evolutions of the frequency shift and the dissipation shift for PEG-8000 aqueous solution on the DOPC SLB at weight fractions of 0.1, 0.5, 1.0, 2.0, 5.0, 10.0, and 20.0% (the data shown are for the third overtone). Upon PEG solution pumping into the chamber, both resonance frequency and energy dissipation shifted from the initial baseline. Both $\Delta f_n/n$ and ΔD_n signals reached plateau values in about 2−3 min. However, after rinsing the chamber with water, both signals went back to 0 quickly, indicating no irreversible adsorption of PEG on the SLB. This process is the same for all concentrations, except that the plateau values of $\Delta f_n/n$ and ΔD_n are more pronounced with increasing concentration. Varying the molecular weight of PEG resulted in the same behavior (Figure 3). It should be noted that the signals for 0.1% PEG-8000 solution are rather small with $\Delta f_n/n = -(0.92 \pm 0.12)$ Hz and $\Delta D_n = (1.2 \pm 0.05) \times 10^{-6}$. At PEG concentration below 0.01%, the signals cannot be distinguished from the noise level (data not shown), indicating no detectable adsorption of PEG on the DOPC SLB in our QCM-D. It had been reported that the nonspecific adsorption of PEG-6000 on silicon oxide (at concentrations below 0.01%) was very small (with a large equilibrium dissociation constant $K_D = 2 \times 10^{-5}$ mol/L, or 0.012%) by using a 55 MHz wireless−electrodeless QCM,[21] which is more sensitive to detect adsorption than the 5 MHz QCM used in the present study (the limit of detection scales with f_0^{-1} in air and $f_0^{-1/2}$ in liquid[19]). We compared the adsorption behavior of PEG on the SLB with that on the bare silicon oxide substrate. It was found that both $-\Delta f_n/n$ and ΔD_n signals in the presence of PEG solutions on the SLB are smaller than those on the bare silicon oxide at the same PEG

DOI: 10.1021/acs.macromol.5b00095
Macromolecules XXXX, XXX, XXX−XXX

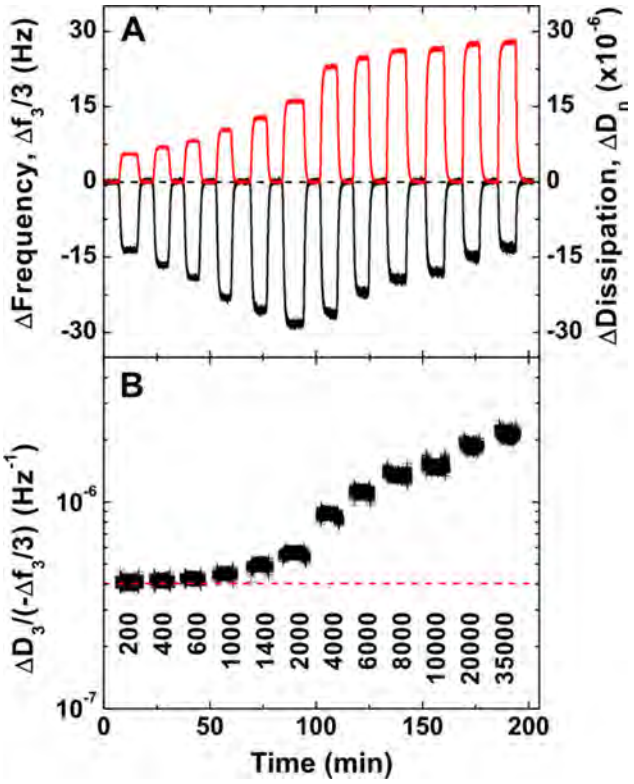

Figure 3. QCM-D signals for a series of subsequent experiments, in which the SLB was exposed to 2.0% PEG aqueous solution with different molecular weights. The signals from left to right are for PEG with molecular weight of 200, 400, 600, 1000, 1400, 2000, 4000, 6000, 8000, 10 000, 20 000, and 35 000, respectively. (A) and (B) are the frequency shift $\Delta f_3/3$ (black curve) and the dissipation shift ΔD_3 (red curve) and their ratio $\Delta D_3/(-\Delta f_3/3)$, respectively. The red dashed line is the theoretical value of $\Delta D_3/(-\Delta f_3/3) = 2/f_0$ for Newtonian fluids.

concentration between 0.1% and 1.0%, indicating the reversible adsorption of PEG on the resonator surface is successfully eliminated by the SLB coating. Previous QCM-D studies by Zhang et al. using the same 5 MHz resonator also found that PEG with a molecular weight of 5000 did not adsorb to the SLB, but PEG with enough hydrophobic end groups did adsorb to the bilayer.[38] The SLB plays the role of a nonadsorbing interface for PEG molecules, in agreement with the literature that PEG is depleted from lipid bilayers.[23−25] The effect of depletion on viscosity of PEG solution is arguably small;[25] therefore, both the frequency shifts and the dissipation shifts should primarily reflect changes in the solution properties, as shown below.

For a quartz resonator in contact with a Newtonian fluid, the frequency shift and the dissipation shift are[13−16]

$$-\frac{\Delta f_n}{n} = n^{-1/2} f_0^{3/2} \left(\frac{\eta_l \rho_l}{\pi \mu_q \rho_q}\right)^{1/2} \tag{2}$$

and

$$\Delta D_n = 2n^{-1/2} f_0^{1/2} \left(\frac{\eta_l \rho_l}{\pi \mu_q \rho_q}\right)^{1/2} \tag{3}$$

where η_l and ρ_l are the solution viscosity and density, respectively. We have studied the frequency shift and dissipation shift for sucrose solutions in contact with the DOPC SLB (Supporting Information Figures S1−S3). Both $-\Delta f_n/n$ and ΔD_n showed good agreement with eqs 2 and 3, and the obtained viscosity agreed very well with the bulk solution viscosity measured by a rheometer. Therefore, forming a SLB on the quartz resonator does not prevent it as a sensor for fluid viscosity and density. Instead, the bilayer served as a rigid nonadsorbing interface to prevent the nonspecific adsorption between the bare silicon oxide substrate with the solutions in the chamber, and the resonator can be used to study the viscosity and density of the Newtonian fluids. According to eqs 2 and 3, the ratio between the dissipation shift and the frequency shift is

$$\frac{\Delta D_n}{-\Delta f_n/n} = \frac{2}{f_0} \tag{4}$$

which is 4.04×10^{-7} Hz^{-1} for $f_0 = 4.95$ MHz. However, a large value of 1.3×10^{-6} Hz^{-1} for PEG-8000 is observed (Figure 2B), indicating that PEG with molecular weight of 8000 shows non-Newtonian behavior in the frequency range of QCM-D and that eqs 2 and 3 are not applicable.

QCM-D measurements for PEG over a broad molecular weight ranging from 200 up to 35 000 were performed. Figure 3 shows the typical QCM-D measurement for dilute aqueous solutions with 2.0% PEG of different molecular weight on the DOPC SLB. No irreversible adsorption of PEG solution on the SLB was found over such a broad molecular weight range. The ratio $\Delta D_n/(-\Delta f_n/n)$ for PEG with molecular weight 200, 400, 600, and 1000 is close to the theoretical value of $2/f_0 = 4.04 \times 10^{-7}$ Hz^{-1} for Newtonian fluids, and it increases with molecular weight to 2.1×10^{-6} Hz^{-1} for PEG-35000. Therefore, the elastic property of PEG solution is getting stronger for higher molecular weight PEG.

For a viscoelastic fluid in contact with an oscillating quartz resonator,[18,19] its complex-valued viscosity as obtained from the frequency shift and the dissipation shift leads to the dynamic viscosity

$$\eta'(\omega) = -\frac{\pi \rho_q \mu_q}{\rho_l f_n} \frac{\Delta f_n \Delta \Gamma_n}{f_0^2} \tag{5}$$

and the storage viscosity

$$\eta''(\omega) = \frac{1}{2} \frac{\pi \rho_q \mu_q}{\rho_l f_n} \frac{\Delta \Gamma_n^2 - \Delta f_n^2}{f_0^2} \tag{6}$$

where the shift of the half-bandwidth $\Delta \Gamma_n = \Delta D_n f_n/2$ with $f_n = nf_0$ the frequency at each overtone n. Note that the complex viscosities are functions of the angular frequency $\omega = 2\pi f_n$. Here one assumes that the SLB is rigid, which is justified by the value of nearly zero for the dissipation of the SLB (Figure 1A). A related version had been derived by Mason et al. for torsional resonator.[8] A Voigt model has also been developed to correlate the QCM-D data with the viscoelasticity of the overlayer.[17] It was found that the above two procedures end up with the same results (Supporting Information), which will be reported in the next section.

Viscoelasticity of PEG Solutions Probed by QCM-D. When we vary the molecular weight of PEG for fixed PEG concentration, the quantities $\Delta f_n/n$ and ΔD_n change non-monotonically with molecular weight. This nonmonotonic behavior is more clearly seen in Figure 4, where both $-\Delta f_n/n$ and ΔD_n are plotted as functions of PEG molecular weight.

DOI: 10.1021/acs.macromol.5b00095
Macromolecules XXXX, XXX, XXX−XXX

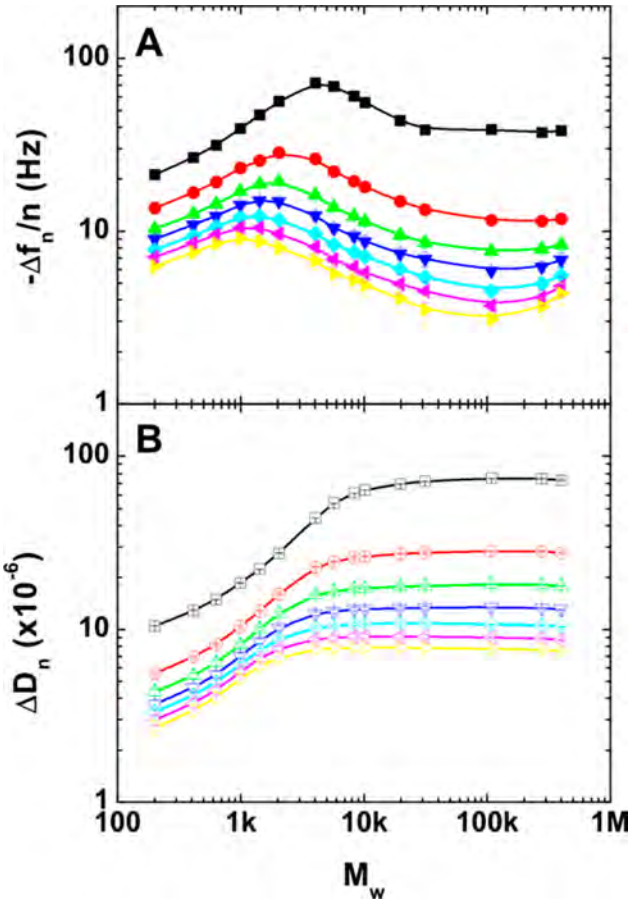

Figure 4. Molecular weight dependence of (A) the frequency shift $-\Delta f_n/n$ and (B) the dissipation shift ΔD_n for 2.0% PEG/PEO aqueous solution on a SLB of DOPC. The values from top to bottom are for overtone number n = 1, 3, 5, 7, 9, 11, and 13, respectively.

Both $-\Delta f_n/n$ and ΔD_n are increasing with molecular weight in the low-M_w region but behave differently in the high-M_w region: a peak for $-\Delta f_n/n$ is observed followed by a decrease to a plateau value at $M_w \geq 35\,000$, while ΔD_n is continuously increasing with M_w to a plateau value at $M_w \geq 35\,000$. Another three PEO samples with higher M_w were examined to show indeed both $-\Delta f_n/n$ and ΔD_n reach plateau values in the high-M_w range. It is interesting to note that both the frequency shift $-\Delta f_n/n$ and the dissipation shift ΔD_n are strongly dependent on the overtone number n: both signals are getting lower with increasing overtone number n; the M_w at the peak for $-\Delta f_n/n$ and at the transition point for ΔD_n are getting lower for higher overtone number n. These observations indicated that the elastic properties are getting stronger at either increasing M_w or higher frequency.

Using eqs 5 and 6, we calculate the complex viscosities of all PEG/PEO solutions. Figure 5 shows the dynamic viscosity η' and storage viscosity η'' for 2.0% PEG/PEO aqueous solution obtained from QCM-D. Both viscosities increase with increasing M_w until a plateau value is reached. There seems to be a small peak for η' before it comes to the plateau region, while η'' is increasing monotonically with M_w up to the plateau region. In the low-M_w regime with $200 \leq M_w \leq 1000$ (for n = 1, the upper limit is shifting to low-M_w region for higher n), it was found that the storage viscosity $\eta'' \approx 0$ and the dynamic viscosity $\eta' \approx \eta$ where η is the bulk solution viscosity measured by a rheometer, corresponding to the behavior of a Newtonian

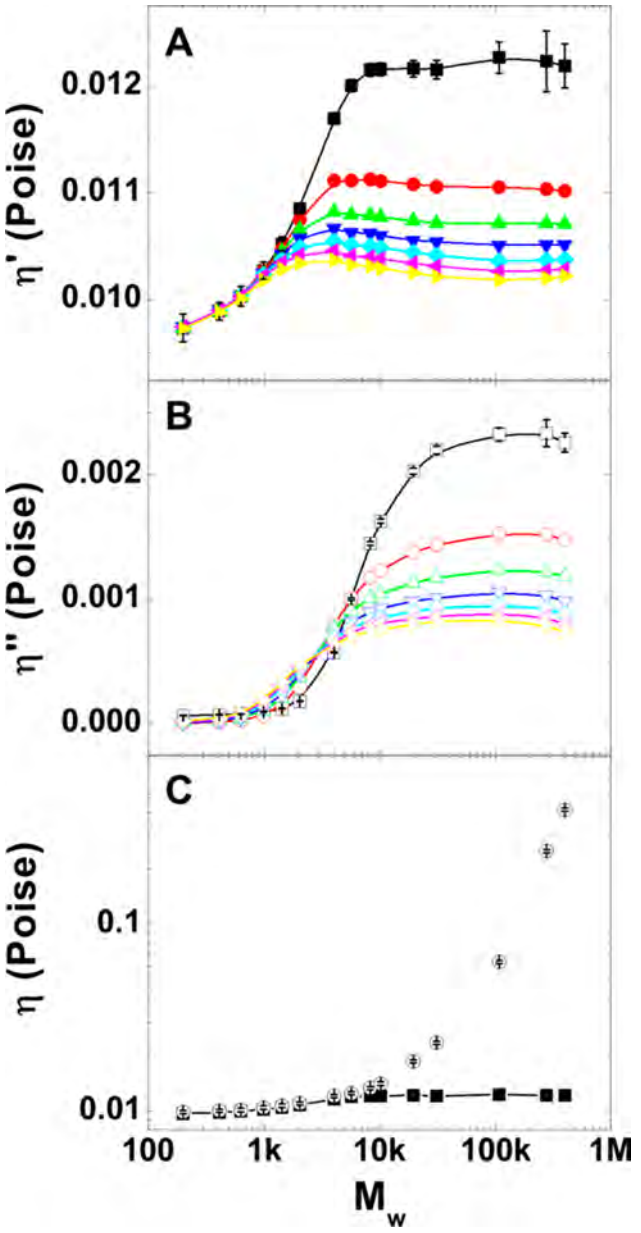

Figure 5. Molecular weight dependence of (A) the dynamic viscosity η' and (B) the storage viscosity η'' for 2.0% PEG/PEO aqueous solution obtained from QCM-D. The values from top to bottom are for overtone number n = 1, 3, 5, 7, 9, 11, and 13, respectively. (C) Viscosity η of 2% PEG/PEO solution measured by a rheometer under steady shear flow (open circles) is compared with the dynamic viscosity η' obtained from the first overtone (solid squares).

fluid. Both $-\Delta f_n/n$ and ΔD_n show a scaling law as n with exponents of $-1/2$ (Supporting Information Figure S4) as expected from eqs 2 and 3. In the high-M_w regime, PEG solutions show non-Newtonian behavior with $\eta'' \neq 0$ and $\eta' < \eta$. Both $-\Delta f_n/n$ and ΔD_n scale as n with exponents smaller than $-1/2$, which is another indication of non-Newtonian behavior. The M_w values for the crossover point between the two regimes shift toward smaller values for higher frequencies.

The shear modulus contributed from the polymer can be calculated via $G' = \omega\eta''$ and $G'' = \omega(\eta' - \eta_s)$, where G' is the storage modulus, G'' is the loss modulus, and η_s is the solvent viscosity. In Figure 6, we plot the reduced storage modulus $G'M_w/(cRT)$ and reduced loss modulus $G''M_w/(cRT)$ as

DOI: 10.1021/acs.macromol.5b00095
Macromolecules XXXX, XXX, XXX−XXX

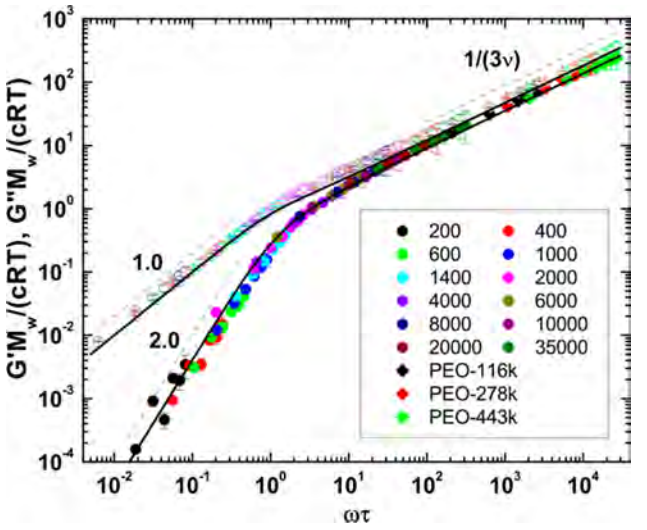

Figure 6. Reduced storage modulus $G'M_w/(cRT)$ (solid symbols) and loss modulus $G''M_w/(cRT)$ (open symbols) for all PEG (circles) and PEO (diamonds) samples. The solid curves are the predictions of the Zimm model with the excluded volume exponent $\nu = 0.565$. The dashed lines are guides to the eyes with the theoretical scaling exponents of 2.0 for $G'M_w/(cRT)$ and 1.0 for $G''M_w/(cRT)$ in the region of $\omega\tau \ll 1$, and $1/(3\nu) = 0.590$ for both modulus in the region of $\omega\tau \gg 1$.

functions of $\omega\tau$ for all PEG/PEO samples of different molecular weight M_w.[1,6,39] Here c is the polymer mass concentration, R is the gas constant, T is the absolute temperature, and τ is the Zimm relaxation time as given by[6]

$$\tau = 0.325\frac{\eta_s \bar{R}^3}{k_B T} \tag{7}$$

where k_B is the Boltzmann constant and $\bar{R}$ is the end-to-end distance of polymer with $\bar{R} = 6^{1/2}R_g$. The radius of gyration R_g can be obtained from its molecular weight according to the scaling relation of $R_g \sim M_w^{\nu}$. Here we use the relation of R_g (nm) $= 0.0215M_w^{0.583}$ for high molecular weight PEG/PEO samples.[40] While for PEG with $M_w < 2000$, R_g (nm) $= 0.0405M_w^{0.50}$ estimated from viscosity measurement was employed.[41,42] Below we will show that the excluded volume exponent ν can be deduced from our data, which is close to the above values.

In Figure 6, we also plot the Zimm model predictions of the storage and loss modulus for dilute solutions of linear polymer chains:[39,43]

$$\frac{G'M_w}{cRT} = \frac{\omega\tau \sin[(1 - 1/(3\nu))\arctan(\omega\tau)]}{[1 + (\omega\tau)^2]^{(1-1/(3\nu))/2}} \tag{8}$$

$$\frac{G''M_w}{cRT} = \frac{\omega\tau \cos[(1 - 1/(3\nu))\arctan(\omega\tau)]}{[1 + (\omega\tau)^2]^{(1-1/(3\nu))/2}} \tag{9}$$

It can be seen that the shear modulus data for all samples collapse to single curves, which are very close to the Zimm model predictions with $\nu = 0.565$. In the region of $\omega\tau \ll 1$, the scaling exponents are 2.0 for $G'M_w/(cRT)$ and 1.0 for $G''M_w/(cRT)$. While in the region of $\omega\tau \gg 1$, both modulus had the same scaling exponents of $1/(3\nu) = 0.590$. These results are in excellent agreement with the theoretical Zimm model of linear polymer chains in a good solvent. It indicated that the viscoelastic properties of polymer solution can be obtained from the QCM-D measurement, which is acting as a microrheometer working in oscillation shear mode at high frequency. It should be noted that the amplitude of the oscillation motion is no more than a few nanometers, ensuring the measurements of the linear viscoelasticity by QCM-D.[18,19]

Taking a closer look into Figure 6, we find that the data for the intermediate range of $\omega\tau$ seem to be slightly deviating from the Zimm model for a good solvent with $\nu = 0.565$. A change to $\nu = 0.50$ fits the data perfectly. Since these data are in the low molecular weight range, the excluded volume effect is small due to the finite size of the polymer, and $\nu = 0.50$ is expected. Below we deduce the excluded volume exponent ν from our measurements (Figure 7).

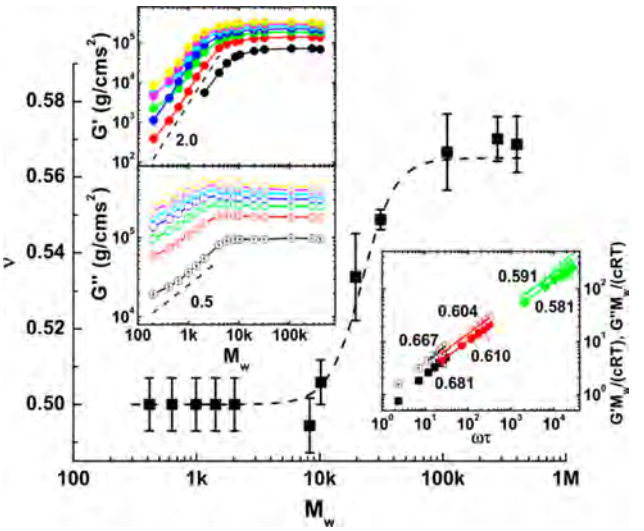

Figure 7. Excluded volume scaling exponent ν as a function of molecular weight of PEG/PEO samples. The dashed line is a fitting to the data. The left insets show the molecular weight dependence of the storage modulus G' and loss modulus G''. The values from bottom to top are for overtone number $n = 1$, 3, 5, 7, 9, 11, and 13, respectively. The dashed lines are guides to the eyes with scaling exponents of 2.0 for G' and 0.5 for G''. The right inset shows the reduced storage modulus $G'M_w/(cRT)$ (solid symbols) and loss modulus $G''M_w/(cRT)$ (open symbols) for PEG-8000 (squares), PEG-35000 (circles), and PEO-443k (diamonds). The solid lines are fittings of the data in the region of $\omega\tau > 10$ to scaling laws, and the obtained exponents are listed nearby.

According to eqs 7−9, in the region of $\omega\tau \ll 1$, one has

$$G' \sim \frac{(\omega\tau)^2}{M_w} \sim M_w^{6\nu-1} \tag{10a}$$

and

$$G'' \sim \frac{\omega\tau}{M_w} \sim M_w^{3\nu-1} \tag{10b}$$

while in the region of $\omega\tau \gg 1$, one obtains

$$G' \sim \frac{(\omega\tau)^{1/(3\nu)}}{M_w} \sim M_w^0 \tag{11a}$$

and

$$G'' \sim \frac{(\omega\tau)^{1/(3\nu)}}{M_w} \sim M_w^0 \tag{11b}$$

DOI: 10.1021/acs.macromol.5b00095
Macromolecules XXXX, XXX, XXX−XXX

In the left insets of Figure 7, G' and G'' are plotted as functions of PEG/PEO molecular weight. In the region of $\omega\tau \ll 1$ for $400 \leq M_w \leq 2000$ (n = 1 and 3), one finds $G' \sim M_w^{2.03\pm0.05}$ and $G'' \sim M_w^{0.49\pm0.02}$, which lead to $\nu = 0.500 \pm 0.007$ for PEG with $400 \leq M_w \leq 2000$. PEG-200 shows slightly lower exponents since it contains only four monomers, which agrees with the previous viscosity measurements.[41,42] For PEG-4000, the lowest value of $\omega\tau$ is 0.66 for n = 1, already outside the region of $\omega\tau \ll 1$, so one cannot estimate its ν. In the region of $\omega\tau \gg 1$ ($M_w \geq 20\,000$ for n = 1), both G' and G'' are indeed independent of molecular weight.

On the other hand, in the high molecular weight region with $\omega\tau \gg 1$, we can fit the data in Figure 6 for each sample individually with $G'M_w/cRT \sim (\omega\tau)^{1/(3\nu)}$ and $G''M_w/cRT \sim (\omega\tau)^{1/(3\nu)}$. In this way, the exponent ν can be deduced from the frequency dependence of the shear moduli for each molecular weight M_w separately. On the contrary, if one derives ν from all the data sets together, the uncertainty of M_w and foreknown ν enter the analysis since they are related to τ by eq 7. The right inset of Figure 7 shows three examples (PEG-8000, PEG-35000, and PEO-443k) of such fittings for $\omega\tau > 10$. From the scaling exponents, we obtain the excluded volume exponent $\nu = 0.494 \pm 0.007$ (PEG-8000), 0.549 ± 0.003 (PEG-35000), and 0.569 ± 0.007 (PEO-443k), respectively. We also perform scaling analysis for the frequency dependence of the complex viscosities according to $(\eta' - \eta_s) \sim \omega^{(1/3\nu-1)}$ and $\eta'' \sim \omega^{(1/3\nu-1)}$, and the obtained ν are the same as we have shown in Figure 7 (Supporting Information Figure S5). It should be noted that for PEG-8000 the scaling analysis is performed in a limited frequency range, corresponding to overtones n = 5−13, since the value of $\omega\tau$ is not big enough for n = 1 and 3. However, the obtained exponent of 0.494 ± 0.007 is still reasonable. In Figure 7, it is shown that the excluded volume exponent ν is gradually increasing from 0.50 ($400 \leq M_w \leq 2000$) to 0.565 ($M_w \geq 100\,000$) with increasing molecular weight. The PEG M_w at the onset of the transition is between 4000 and 8000. Kawaguchi studied the molecular weight dependence of the intrinsic viscosity of PEG/PEO in water[42] and also found a transition for the exponent α in the scaling law $[\eta] \sim M_w^{\alpha}$; they observed 0.50 for $M_w \leq 6000$ and 0.679 for $M_w \geq 6000$. Not only the M_w at the transition point is close, but also the exponents agree well by considering the relation $\alpha = 3\nu - 1$. Eshuis et al. studied the dynamic moduli of PEG solutions by a torsional resonator up to 250 kHz;[44] a shifting procedure for two monodisperse PEG samples with M_w of 12 800 and 29 300 gave ν = 0.565 at 20 °C and ν = 0.54 at 30 °C, also in accord with our results at 24 °C. It should be noted that the current method from viscoelasticity of polymer solution can give the value of ν at each molecular weight, without the need to do scaling analysis on the molecular weight. For linear long polymer chains in a good solvent, where excluded volume effects are appreciable, polymer physics theory predicted $R_g \sim M_w^{\nu}$ with ν = 0.588.[6] However, for short chains with a size below the thermal blob size, the self-avoidance is not significant, and the chain assumes an ideal random-walk configuration.[39] Therefore, a certain polymer in a good solvent can display an ideal-to-real crossover with increasing chain length; the crossover reflects the size of the thermal blob. Saleh et al. had performed single-molecule elasticity measurements of PEG in water;[45] they found the thermal blob size of PEG to be 6 nm and the onset of the excluded volume to be roughly 100 ethylene oxide units, i.e., with $M_w \sim 4400$. Our results are in good agreement with the outcome of this sophisticated experiment.

Therefore, one can conclude that the shifts in the resonance frequency and the energy dissipation factor in the QCM-D measurements of PEG solutions on the rigid resonator-supported lipid bilayer are due to the viscoelastic properties of the polymer solutions. QCM-D can be employed to study the viscoelastic properties of polymer solution at megahertz frequency, which is very useful for short polymer chains and is complementary to the rotational rheometer and torsional resonator rheometer working in the lower frequency regimes. QCM-D measurements are performed over tens of milliseconds and, thus, over time scales that are much longer than the period of the oscillatory motion, ensuring that the systems can reach a steady state. Therefore, these measurements should probe the viscoelasticity of polymer solution in the megahertz frequency range in a rapid and accurate way. The use of a SLB as an intermediate layer between the resonator and the bulk liquid to be studied is beneficial with regard to viscoelasticity measurements because the SLB provides a rigid nonadsorbing interface. One might also passivate the resonator with other inert layers to study the viscoelasticity of different polymer species.

CONCLUSIONS

PEG solutions of different molecular weights at various concentrations were exposed to supported lipid bilayers of DOPC and studied by QCM-D. No adsorption of PEG molecules could be detected on the bilayer. The viscoelastic properties of the PEG solution were obtained from the shifts in the resonance frequency and the energy dissipation factor due to the presence of PEG solution at the resonator. Good agreement of the viscoelastic properties of PEG solution with the Zimm model for linear polymer chains in a good solvent was found, as shown in Figure 6. The excluded volume scaling exponent ν for PEG/PEO in water shows an ideal-to-real crossover with increasing molecular weight, i.e., from ν = 0.50 for short chains to ν = 0.565 for long chains, as demonstrated in Figure 7. The onset of the excluded volume effect of PEG in water, a good solvent, occurs at molecular weight between 4000 and 8000.

ASSOCIATED CONTENT

Supporting Information

Molecular weight distribution of PEG and PEO samples, relations of the frequency shift and the bandwidth shift with the complex viscosity, viscosity of sucrose solutions on the DOPC SLB, scaling laws for the frequency shift, the dissipation factor shift, and the complex viscosities of PEG/PEO solutions on the normalized frequency. This material is available free of charge via the Internet at http://pubs.acs.org.

AUTHOR INFORMATION

Corresponding Authors

*E-mail xlji@ciac.ac.cn (X.J.).
*E-mail yonggang@ciac.ac.cn (Y.L.).

Notes

The authors declare no competing financial interest.

ACKNOWLEDGMENTS

Z.Z. thanks Erik Reimhult for insightful discussions at the early stage of the experiment. This work is supported by the grants of the National Natural Science Foundation of China (21274147),

DOI: 10.1021/acs.macromol.5b00095
Macromolecules XXXX, XXX, XXX−XXX

the Natural Science Foundation of Jilin Province, China (201215093), and the MPG-CAS Partner Group Program.

REFERENCES

(1) Ferry, J. D. *Viscoelastic Properties of Polymers*; Wiley: New York, 1980.
(2) Larson, R. G. *The Structure and Rheology of Complex Fluids*; Oxford University Press: New York, 1999.
(3) Rouse, P. E. *J. Chem. Phys.* **1953**, *21*, 1272−1280.
(4) Zimm, B. H. *J. Chem. Phys.* **1956**, *24*, 269−278.
(5) Morse, D. C. *Macromolecules* **1998**, *31*, 7044−7067.
(6) Doi, M.; Edwards, S. F. *The Theory of Polymer Dynamics*; Clarendon Press: Oxford, 1986.
(7) Dasgupta, B. R.; Tee, S. Y.; Crocker, J. C.; Frisken, B. J.; Weitz, D. A. *Phys. Rev. E* **2002**, *65*, 051505.
(8) Mason, W. P. *Piezoelectric Crystals and Their Applications to Ultrasonics*; Van Nostrand: Princeton, 1948.
(9) Stokich, T. M.; Radtke, D. R.; White, C. C.; Schrag, J. L. *J. Rheol.* **1994**, *38*, 1195−1210.
(10) Yoshizaki, H. *Polym. J.* **1993**, *25*, 553−559.
(11) Fritz, G.; Pechhold, W.; Willenbacher, N.; Wagner, N. J. *J. Rheol.* **2003**, *47*, 303−319.
(12) Sauerbrey, G. *Z. Phys.* **1959**, *155*, 206−222.
(13) Kanazawa, K. K.; Gordon, J. G. *Anal. Chem.* **1985**, *57*, 1770−1771.
(14) Kanazawa, K. K.; Gordon, J. G. *Anal. Chim. Acta* **1985**, *175*, 99−105.
(15) Rodahl, M.; Kasemo, B. *Sens. Actuators, A* **1996**, *54*, 448−456.
(16) Saluja, A.; Kalonia, D. S. *AAPS PharmSciTech* **2004**, *5*, 68−81.
(17) Voinova, M. V.; Rodahl, M.; Jonson, M.; Kasemo, B. *Phys. Scr.* **1999**, *59*, 391−396.
(18) Johannsmann, D. *Phys. Chem. Chem. Phys.* **2008**, *10*, 4516−4534.
(19) Johannsmann, D. *The Quartz Crystal Microbalance in Soft Matter Research: Fundamentals and Modeling*; Springer: Berlin, 2015.
(20) Wang, P.; Fang, J.; Qin, S.; Kang, Y.; Zhu, D. *J. Phys. Chem. C* **2009**, *113*, 13793−13800.
(21) Ogi, H.; Fukunishi, Y.; Nagai, H.; Okamoto, K.; Hirao, M.; Nishiyama, M. *Biosens. Bioelectron.* **2009**, *24*, 3148−3152.
(22) Keller, C. A.; Kasemo, B. *Biophys. J.* **1998**, *75*, 1397−1402.
(23) Kuhl, T.; Guo, Y.; Alderfer, J. L.; Berman, A. D.; Leckband, D.; Israelachvili, J.; Hui, S. W. *Langmuir* **1996**, *12*, 3003−3014.
(24) Armstrong, J. K.; Wenby, R. B.; Meiselman, H. J.; Fisher, T. C. *Biophys. J.* **2004**, *87*, 4259−4270.
(25) Kuhl, T. L.; Berman, A. D.; Hui, S. W.; Israelachvili, J. N. *Macromolecules* **1998**, *31*, 8258−8263.
(26) Li, Y.; Lipowsky, R.; Dimova, R. *Proc. Natl. Acad. Sci. U. S. A.* **2011**, *108*, 4731−4736.
(27) Terasawa, H.; Nishimura, K.; Suzuki, H.; Matsuura, T.; Yomo, T. *Proc. Natl. Acad. Sci. U. S. A.* **2012**, *109*, 5942−5947.
(28) Lipowsky, R.; Döbereiner, H. G. *Europhys. Lett.* **1998**, *43*, 219−225.
(29) Mertin, O.; Dimova, R. *Langmuir* **2011**, *27*, 5506−5515.
(30) Cho, N. J.; Frank, C. W.; Kasemo, B.; Höök, F. *Nat. Protoc.* **2010**, *5*, 1096−1106.
(31) Richter, R. P.; Brisson, A. R. *Biophys. J.* **2005**, *88*, 3422−3433.
(32) Reimhult, E.; Zach, M.; Hook, F.; Kasemo, B. *Langmuir* **2006**, *22*, 3313−3319.
(33) Richter, R. P.; Berat, R.; Brisson, A. R. *Langmuir* **2006**, *22*, 3497−3505.
(34) Richter, R.; Mukhopadhyay, A.; Brisson, A. *Biophys. J.* **2003**, *85*, 3035−3047.
(35) Jackman, J. A.; Choi, J. H.; Zhdanov, V. P.; Cho, N. J. *Langmuir* **2013**, *29*, 11375−11384.
(36) Andrecka, J.; Spillane, K. M.; Ortega-Arroyo, J.; Kukura, P. *ACS Nano* **2013**, *7*, 10662−10670.
(37) Seifert, U.; Lipowsky, R. *Phys. Rev. A* **1990**, *42*, 4768−4771.
(38) Liu, G.; Fu, L.; Zhang, G. *J. Phys. Chem. B* **2009**, *113*, 3365−3369.
(39) Rubinstein, M.; Colby, R. H. *Polymer Physics*; Oxford University Press: New York, 2003.
(40) Devanand, K.; Selser, J. C. *Macromolecules* **1991**, *24*, 5943−5947.
(41) Kuga, S. *J. Chromatogr.* **1981**, *206*, 449−461.
(42) Kawaguchi, S.; Imai, G.; Suzuki, J.; Miyahara, A.; Kitano, T.; Ito, K. *Polymer* **1997**, *38*, 2885−2891.
(43) Colby, R. H. *Rheol. Acta* **2010**, *49*, 425−442.
(44) Eshuis, A.; Mijnlieff, P. F. *Polymer* **1986**, *27*, 1951−1957.
(45) Dittmore, A.; McIntosh, D. B.; Halliday, S.; Saleh, O. A. *Phys. Rev. Lett.* **2011**, *107*, 148301.

DOI: 10.1021/acs.macromol.5b00095
Macromolecules XXXX, XXX, XXX−XXX

Supporting Information

Viscoelasticity of Poly(ethylene glycol) Solutions on Supported Lipid Bilayers via Quartz Crystal Microbalance with Dissipation

Ziliang Zhao,[†,§] Xiangling Ji,[*,†] Rumiana Dimova,[‡] Reinhard Lipowsky,[‡] Yonggang Liu[*,†,‡]

[†] State Key Laboratory of Polymer Physics and Chemistry, Changchun Institute of Applied Chemistry, Chinese Academy of Sciences, 130022 Changchun, China

[‡] Department of Theory and Bio-Systems, Max Planck Institute of Colloids and Interfaces, Science Park Golm, 14424 Potsdam, Germany

[§] University of Chinese Academy of Sciences, 100049 Beijing, China

[*] Corresponding author: xlji@ciac.ac.cn (X.J.); yonggang@ciac.ac.cn (Y.L.)

Molecular Weight Distribution of PEG and PEO Samples. The molecular weights of 12 PEG samples and 3 PEO samples were determined by a gel permeation chromatography equipped with either two PL aquagel-OH 30 or two PL aquagel-OH mixed-H columns (7.5×300mm) with refractive index detection. Water containing 0.02% NaN_3 was used as the eluent at a flow rate of 1.0 mL/min. The columns were calibrated with narrow PEG/PEO standards from Polymer Laboratories Ltd. Table S1 summarized the molecular weight data of these PEG and PEO samples.

Relations of the Frequency Shift and the Bandwidth Shift with the Complex Viscosity. Rearrangements of eqs (5) and (6) in the main text lead to the frequency shift

$$\Delta f_n = -\sqrt{\frac{n}{\pi\rho_q\mu_q}} f_0^{3/2} \sqrt{\rho_l\left(\sqrt{\eta'^2+\eta''^2}-\eta''\right)} \qquad \text{(S1)}$$

and the bandwidth shift

$$\Delta\Gamma_n = \sqrt{\frac{n}{\pi\rho_q\mu_q}} f_0^{3/2} \sqrt{\rho_l\left(\sqrt{\eta'^2+\eta''^2}+\eta''\right)} \qquad \text{(S2)}$$

On the other hand, the Voigt model relates the viscosity and elasticity of the overlay with the frequency shift and the dissipation shift via[1]

$$\Delta f_n = -\frac{1}{2\pi\rho_q h_q}\sqrt{\frac{\rho_l}{2}}\left[\eta\omega\sqrt{\frac{\sqrt{\mu^2+\eta^2\omega^2}+\mu}{\mu^2+\eta^2\omega^2}}-\mu\sqrt{\frac{\sqrt{\mu^2+\eta^2\omega^2}-\mu}{\mu^2+\eta^2\omega^2}}\right] \qquad \text{(S3)}$$

$$\Delta D_n = \frac{1}{\pi f_n\rho_q h_q}\sqrt{\frac{\rho_l}{2}}\left[\eta\omega\sqrt{\frac{\sqrt{\mu^2+\eta^2\omega^2}-\mu}{\mu^2+\eta^2\omega^2}}+\mu\sqrt{\frac{\sqrt{\mu^2+\eta^2\omega^2}+\mu}{\mu^2+\eta^2\omega^2}}\right] \qquad \text{(S4)}$$

where $h_q = (\mu_q/\rho_q)^{1/2}/2f_0$. After renaming the variables ($\mu \rightarrow \eta''\omega$, $\eta \rightarrow \eta'$),[2] the frequency shift can be written as

$$\Delta f_n = -\sqrt{\frac{n}{\pi\rho_q\mu_q}} f_0^{3/2}\sqrt{\rho_l}\left[\eta'\sqrt{\frac{\sqrt{\eta'^2+\eta''^2}+\eta''}{\eta'^2+\eta''^2}} - \eta''\sqrt{\frac{\sqrt{\eta'^2+\eta''^2}-\eta''}{\eta'^2+\eta''^2}}\right] \quad \text{(S5)}$$

and the bandwidth shift, $\Delta\Gamma_n = \Delta D_n f_n/2$, is

$$\Delta\Gamma_n = \sqrt{\frac{n}{\pi\rho_q\mu_q}} f_0^{3/2}\sqrt{\rho_l}\left[\eta'\sqrt{\frac{\sqrt{\eta'^2+\eta''^2}-\eta''}{\eta'^2+\eta''^2}} + \eta''\sqrt{\frac{\sqrt{\eta'^2+\eta''^2}+\eta''}{\eta'^2+\eta''^2}}\right] \quad \text{(S6)}$$

Apparently eqs (S1)-(S2) seem to take concise albeit different forms with eqs (S5)-(S6). In these equations, the pre-factor $K = \sqrt{\frac{n}{\pi\rho_q\mu_q}} f_0^{3/2}$ is a constant for each overtone. By assuming $\eta' = k\eta''$ with k the ratio between the dynamic viscosity and storage viscosity, these equations can be simplified to functions of η'' and k

$$\Delta f_n = -K\sqrt{\rho_l\eta''}\left[\sqrt{\sqrt{1+k^2}-1}\right] \quad \text{(S7)}$$

$$\Delta\Gamma_n = K\sqrt{\rho_l\eta''}\left[\sqrt{\sqrt{1+k^2}+1}\right] \quad \text{(S8)}$$

$$\Delta f_n = -K\sqrt{\rho_l\eta''}\left[k\sqrt{\frac{\sqrt{1+k^2}+1}{1+k^2}} - \sqrt{\frac{\sqrt{1+k^2}-1}{1+k^2}}\right] \quad \text{(S9)}$$

$$\Delta\Gamma_n = K\sqrt{\rho_l\eta''}\left[k\sqrt{\frac{\sqrt{1+k^2}-1}{1+k^2}} + \sqrt{\frac{\sqrt{1+k^2}+1}{1+k^2}}\right] \quad \text{(S10)}$$

We have plotted the terms in the square bracket as functions of k, and found those from eqs (S7)-(S8) coincide exactly with those from eqs (S9)-(S10). Actually some algebraic calculations show these equations are actually the same, since

$$\left[k\sqrt{\frac{\sqrt{1+k^2}+1}{1+k^2}} - \sqrt{\frac{\sqrt{1+k^2}-1}{1+k^2}}\right]^2 = \sqrt{1+k^2}-1 \quad \text{(S11)}$$

$$\left[k\sqrt{\frac{\sqrt{1+k^2}-1}{1+k^2}}+\sqrt{\frac{\sqrt{1+k^2}+1}{1+k^2}}\right]^2=\sqrt{1+k^2}+1 \qquad \text{(S12)}$$

Therefore we concluded that the procedures from eqs (5) and (6) and the Voigt model gave the same results.

Viscosity of Sucrose Solutions on the DOPC SLB. After forming supported lipid bilayer of DOPC on silicon oxide substrate, the adsorption behavior of sucrose solution was subsequently studied at sucrose weight fraction $w_{sucrose}$ of 0.50, 1.0, 2.0, 5.0, 10.0, 20.0, 25.0, and 50.0%. The resonance frequency and the energy dissipation factor for all 7 harmonics (overtone number n = 1, 3, 5, 7, 9, 11, and 13) were monitored as the sucrose solution pumping into the chamber followed by rinsing with water (Figure S1). The shifts in the resonance frequency and the energy dissipation factor induced by sucrose solution disappear as soon as the sucrose solutions had been rinsed away by water, indicating no irreversible adsorption. The plateau values of the frequency shift and the dissipation shift in the presence of sucrose solution were plotted as a function of the overtone number n, both showing the scaling laws of $-\Delta f_n/n \sim n^{-1/2}$ and $\Delta D_n \sim n^{-1/2}$ (Figure S2). The complex viscosities obtained from QCM-D show the behaviors of typical Newtonian fluids with dynamic viscosity η' = constant and storage viscosity η'' = 0, and the obtained η' agreed well with the bulk solution viscosity measured by a rheometer (Figure S3).

Scaling Laws for the Frequency Shift, the Dissipation Factor Shift, and the Complex Viscosities of PEG/PEO Solutions on the Normalized Frequency. Figure S4 shows the dependence of the frequency shift-$\Delta f_n/n$, the dissipation factor shift ΔD_n on the normalized frequency $\omega\tau$. The scaling exponents decrease from -1/2 for low molecular weight PEG to -0.9 for high molecular weight PEG/PEO. Figure S5 shows the dependence of the polymer contributed complex viscosity on the normalized frequency in the region of $\omega\tau > 10$. The scaling

exponents for high molecular weight PEOs is about -0.41, in accord with the value of $1/(3\nu)-1$ with $\nu = 0.565$.

REFERENCES

1. Voinova, M. V.; Rodahl, M.;Jonson, M.; Kasemo, B. *Phys. Scr.* **1999**, *59*, 391-396.

2. Johannsmann, D. *The Quartz Crystal Microbalance in Soft Matter Research: Fundamentals and Modeling*; Springer: Berlin, 2015.

Table S1. Molecular weight data of PEG and PEO samples.

sample[a]	supplier	M_w (g/mol)	M_n (g/mol)	M_w/M_n
PEG-200	SA[b]	201	183	1.10
PEG-400	SA	414	370	1.12
PEG-600	SA	631	591	1.07
PEG-1000	SA	992	936	1.06
PEG-1400	SA	1430	1350	1.06
PEG-2000	SA	2040	1980	1.03
PEG-4000	SA	4030	3900	1.03
PEG-6000	SA	5720	5430	1.05
PEG-8000	SA	8330	7970	1.05
PEG-10000	SA	10240	9450	1.08
PEG-20000	SA	19600	18160	1.08
PEG-35000	SA	31330	28650	1.09
PEO-116k	PL[c]	108700	99600	1.09
PEO-278k	PL	278700	248400	1.12
PEO-443k	PL	399900	312700	1.28

[a] The numbers in the sample name are weight-average molecular weight M_w as given by suppliers. [b] Sigma-Aldrich. [c] Polymer Laboratories Ltd.

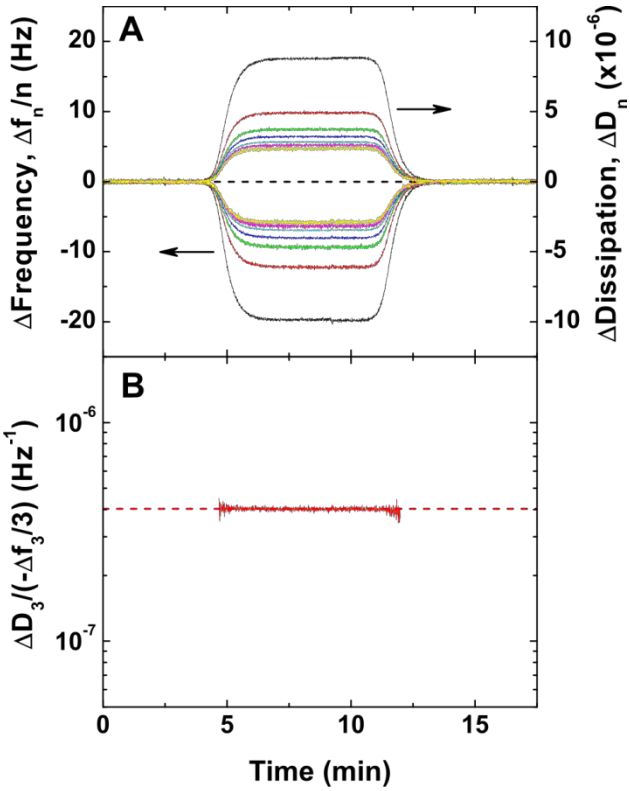

Figure S1. A typical QCM-D measurement for 2.0% sucrose aqueous solution on a SLB of DOPC. (A) Resonance frequency shifts $\Delta f_n/n$ and the energy dissipation shifts ΔD_n for all seven harmonics as a function of time. The frequency signals from bottom to top are for overtone number n = 1, 3, 5, 7, 9, 11, and 13, respectively. The corresponding dissipation signals at each overtone are shown with the same color as frequency. (B) Ratio of the dissipation shift to the frequency shift for the third overtone, $\Delta D_3/(-\Delta f_3/3)$, as a function of time. A constant value very close to the theoretical value of $\Delta D_3/(-\Delta f_3/3) = 2/f_0$ (the red dashed line) was observed.

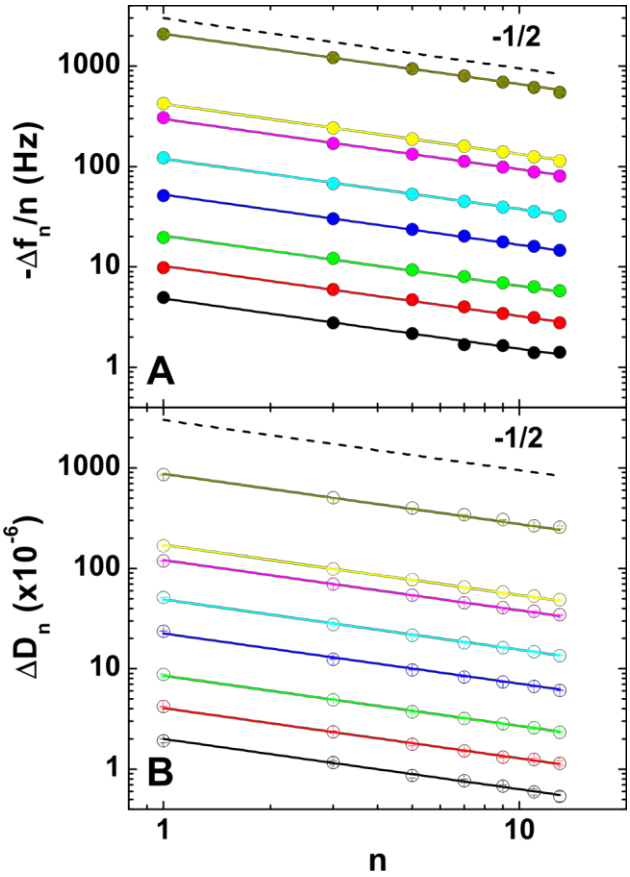

Figure S2. Dependence of (A) the frequency shifts $-\Delta f_n/n$ and (B) the dissipation shifts ΔD_n on the overtone number n. The data from bottom to top are for solution with sucrose weight fraction $w_{sucrose}$ of 0.50, 1.0, 2.0, 5.0, 10.0, 20.0, 25.0, and 50.0%, respectively. The solid lines are fitting to the data with scaling exponents of -1/2 (the dash lines serve as guides to the eyes).

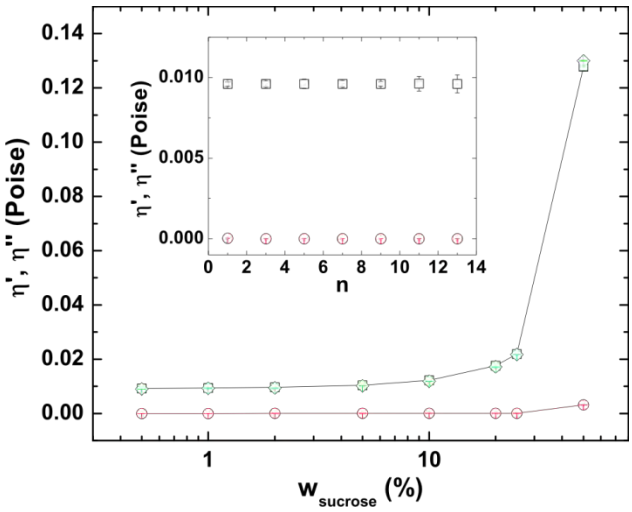

Figure S3. Dynamic viscosity η' (open squares) and storage viscosity η'' (open circles) of sucrose solution obtained from QCM-D as a function of sucrose weight fraction w_{sucrose}. The viscosity η of sucrose solution measured by a rheometer under steady shear flow is also shown (open diamond). The inset shows the complex viscosities of 2.0% sucrose solution for all harmonics from overtone number n = 1 up to 13.

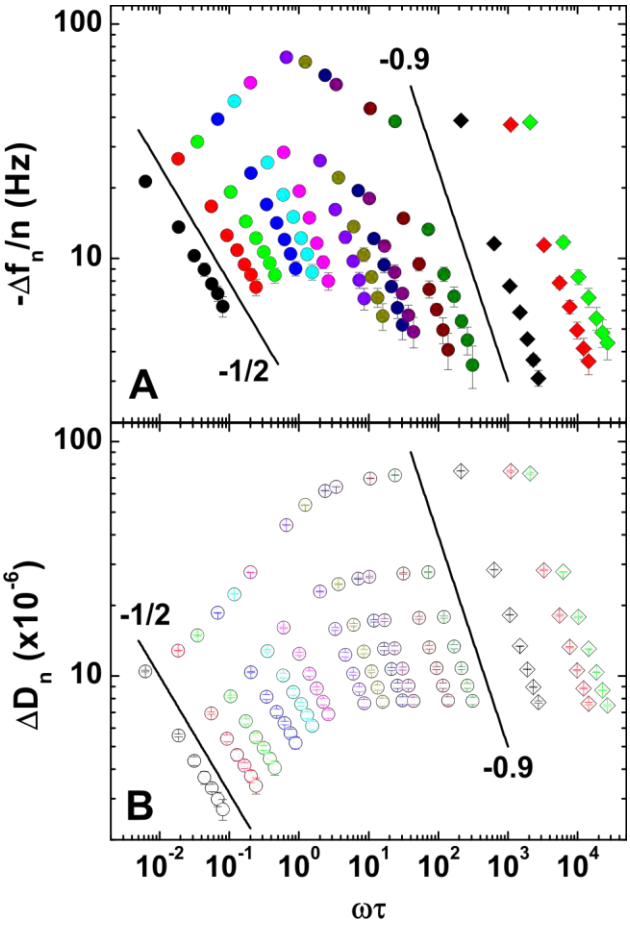

Figure S4. Dependence of (A) the frequency shifts $-\Delta f_n/n$ and (B) the dissipation shifts ΔD_n on $\omega\tau$ for 2.0% PEG/PEO aqueous solution on a SLB of DOPC. The data from left to right are for PEG/PEO with molecular weight of 200, 400, 600, 1000, 1400, 2000, 4000, 6000, 8000, 10000, 20000, 35000, 116000, 278000, and 443000, respectively. The solid lines serve as guides to the eye with scaling exponents of -1/2 for low molecular weight PEG and -0.9 for high molecular weight PEG/PEO.

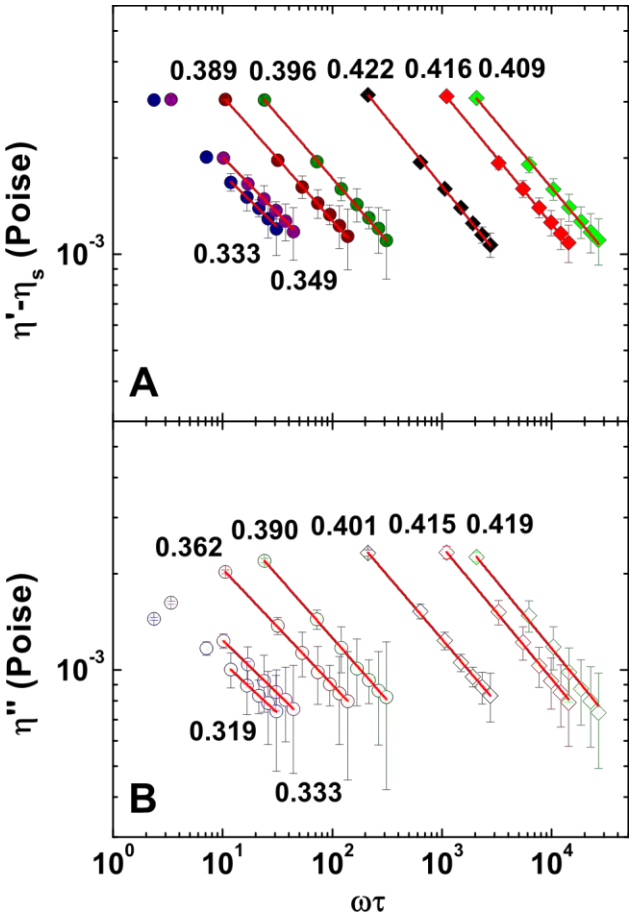

Figure S5. Dependence of polymer contributed dynamic viscosity η'-η_s (A) and storage viscosity η'' (B) on $\omega\tau$ for 2.0% PEG/PEO aqueous solution obtained from QCM-D. The data from left to right are for PEG/PEO with molecular weight of 8000, 10000, 20000, 35000, 116000, 278000, and 443000, respectively. The solid lines are fittings of the data in the region of $\omega\tau > 10$ to scaling laws and the obtained exponents are listed nearby.